Author Manuscript

Accepted for publication in a peer-reviewed journal

NIST National Institute of Standards and Technology • U.S. Department of Commerce

Published in final edited form as:

Anal Bioanal Chem. 2016 November ; 408(27): 7629–7640. doi:10.1007/s00216-016-9844-x.

Practical utilization of spICP-MS to study sucrose density gradient centrifugation for the separation of nanoparticles

Monique E. Johnson[1], **Antonio R. Montoro Bustos**[1], and **Michael R. Winchester**[1]

[1]Material Measurement Laboratory, National Institute of Standards and Technology, 100 Bureau Drive, Gaithersburg, MD 20899-8391, USA

Abstract

Single particle inductively coupled plasma mass spectrometry (spICP-MS) is shown to be a practical technique to study the efficacy of rate-zonal sucrose density gradient centrifugation (SDGC) separations of mixtures of gold nanoparticles (AuNPs) in liquid suspension. spICP-MS enabled measurements of AuNP size distributions and particle number concentrations along the gradient, allowing unambiguous evaluations of the effectiveness of the separation. Importantly, these studies were conducted using AuNP concentrations that are directly relevant to environmental studies (sub ng mL^{-1}). At such low concentrations, other techniques [e.g., dynamic light scattering (DLS), transmission and scanning electron microscopies (TEM and SEM), UV–vis spectroscopy, atomic force microscopy (AFM)] do not have adequate sensitivity, highlighting the inherent value of spICP-MS for this and similar applications. In terms of the SDGC separations, a mixture containing three populations of AuNPs, having mean diameters of 30, 80, and 150 nm, was fully separated, while separations of two other mixtures (30, 60, 100 nm; and 20, 50, 100 nm) were less successful. Finally, it is shown that the separation capacity of SDGC can be overwhelmed when particle number concentrations are excessive, an especially relevant finding in view of common methodologies taken in nanotechnology research.

Keywords

Sucrose density gradient centrifugation; ICP-MS; spICP-MS; Gold nanoparticles

Introduction

The field of nanotechnology has fostered innovations that have facilitated the exponential growth of the incorporation of nanomaterials into consumer products, [1] biomedical

Monique E. Johnson and Antonio R. Montoro Bustos contributed equally to this work.

Electronic supplementary material The online version of this article (doi:10.1007/s00216-016-9844-x) contains supplementary material, which is available to authorized users.

Compliance with ethical standards

NIST disclaimer Certain commercial equipment, instruments and materials are identified in this paper to specify an experimental procedure as completely as possible. In no case does the identification of particular equipment or materials imply a recommendation or endorsement by the National Institute of Standards and Technology nor does it imply that the materials, instruments, or equipment are necessarily the best available for the purpose.

Conflict of interest The authors declare no conflicts of interest.

applications, [2] sensing devices, [3] photovoltaics, [4] and many other forms of technology. Nanoparticles (NPs), defined as nanomaterials with three external dimensions falling in the range from 100 nm down to approximately 1 nm, [5] may have a natural or an anthropogenic origin and can be synthesized in a plethora of shapes and sizes [6–9] with varying compositions. [10–13] Fabricators have placed an emphasis on the synthesis of NPs of uniform and discrete shapes and sizes with low polydispersity in order to achieve well-defined properties and functions. [14] Uniformity in size can be accomplished by adjusting growth parameters during synthesis [15, 16] or by resorting to post-synthesis purification procedures, [17–19] the latter being the preferred choice in many cases due to the efficacy of available size separation techniques. [14]

Among all the methods commonly used for NP separation and purification, [20] centrifugation is usually considered the simplest and most convenient. [21] More specifically, density gradient centrifugation has been utilized to achieve size, shape, and agglomeration/aggregation control. [22] This approach has been applied to the separation/purification of nanomaterials in recent years, but at high concentration levels. An iodixanol gradient was used for the separation of FeCo@C, [14] while a CsCl gradient has been applied to isolate gold NPs, dimers, and trimers. [23] Currently, sucrose, the most prevalently utilized gradient medium, has been applied to separate gold nanorods, [22] carbon nanotubes, [24] titanium dioxide, [25] and gold and silver NPs in plant leaf extracts. [26] In our research group, the real-life application of a sucrose density gradient centrifugation (SDGC) protocol has been recently employed in a bioaccumulation study for the facile separation of AuNPs in *Caenorhabditis elegans* (soil inhabiting nematode species [27]) after 24 h incubation, initiating whole organismal metrology efforts. (Johnson et al. 2016, *to be submitted to ACS Nano*) Typically, the verification of physical separation of different NP sizes in polydispersed mixtures is accomplished with non-quantitative approaches, such as ultraviolet–visible spectroscopy (UV–vis) and transmission electron microscopy (TEM), which are inherently limited to detection at high concentrations (sub μg mL^{-1} levels). However, characterizing and quantifying NPs and NP mixtures under realistic environmental exposure conditions remains a substantial challenge because of the extremely low environmental concentrations of NPs (on the order of pg mL^{-1}) in complex matrices. [28, 29]

Inductively coupled plasma-mass spectrometry (ICP-MS) is considered one of the most versatile elemental techniques, providing rapid multi-elemental analysis and low detection limits (sub pg mL^{-1}) for a large range of samples on a routine basis. Overall, ICP-MS can currently be considered the technique of choice for reliable quantification and elemental characterization of metallic NPs. [30] A relatively recent modification of conventional ICP-MS, which performs “particle by particle” measurements by operating in a time-resolved analysis mode with short detector dwell times, is single particle (sp)ICP-MS, an emergent technique for detecting, characterizing, and quantifying NPs. [31] spICP-MS is presently the only technique which enables the simultaneous acquisition of valuable types of information about metal-containing NPs, such as the elemental composition, size and size distribution, and number concentration at mass fraction levels down to sub pg g^{-1} levels. [32, 33] Moreover, the spICP-MS capability of differentiating between dissolved and particulate forms of an element [34] and its ability to resolve the components of polydispersed samples

containing dissolved ions and NPs of more than one size [35–37] make this an advantageous technique for the advancement of nanotechnology.

The objective of the study reported here is to examine the practical utilization of spICP-MS to study the suitability of rate-zonal SDGC separations of AuNP mixtures at environmentally relevant concentrations, using total Au analysis by conventional ICP-MS as a prescreening tool. Size characterization, quantification, and the contribution of each component of several mixtures, in terms of nanoparticle size and number concentration across the sucrose layers, are investigated. The influence of equal particle number concentration (ePNC) and equal Au mass fraction (eMF) conditions on the efficacy of the separation is explored. These parameters are critical, because the distribution of NPs across layers of different densities is expected to be governed by particle number concentration, although an equal mass fraction scenario is employed in many research efforts.

Finally, we emphasize that the mass fractions of nanoparticles under study are in the environmental range (sub ng g^{-1} levels), meaning that they are in the range in which nanoparticles are typically found in actual, environmental samples. This is extremely important, because of the tendency of many researchers involved in environmental, health, and safety (EHS) studies of nanomaterials to use much higher nanoparticle concentrations. While there may be many reasons, two possible reasons for the use of such high concentrations are to ensure a response in toxicological studies and to make the nanomaterials detectable using typical analytical methods, such as TEM. The use of high concentrations brings into question the real-world significance of conclusions drawn from such work. In the work reported here, spICP-MS enables for the first time the evaluation of the application of SDGC to the separation of NP mixtures at the low levels found in environmental samples, enabling EHS studies at realistic concentration levels. We should also emphasize that the major usefulness of SDGC is that it potentially provides physical separations of the discrete components of mixtures of NPs with different sizes, shapes, and concentrations in a myriad of realistic NP exposure scenarios in a nondestructive way, preserving the separated components for further study. While it would be possible to use spICP-MS alone on an environmental sample to characterize the NPs therein, those NPs would be destroyed in the process. Therefore, we consider that the use of SDGC and spICP-MS in tandem, as described in this paper, provides a capability never before achieved.

Materials and methods

Chemicals

All chemicals were of analytical grade and used as received without further purification. High-purity water (≥18 MΩ · cm resistivity, Millipore) and Optima acids (HNO_3 and HCl, Fisher Scientific) were used in all ICP-MS experiments. A dissolved gold standard solution, National Institute of Standards and Technology (NIST) Standard Reference Material (SRM) 3121, lot number 991806, was used to prepare all dissolved gold standards for instrument calibration. Platinum (NIST SRM 3140, lot number 140930) and indium (NIST SRM 3124a, lot number 991219) standard solutions were used to prepare internal standards for the determination of total Au concentrations. Sucrose (enzyme-grade powder) from Life Technologies (NY, USA) was used as a density gradient medium. Food coloring (green, red,

yellow, and blue) was purchased from a local market. Monodispersed, citrate-stabilized, spherical AuNPs were used. Particles analyzed included commercially available NP suspensions purchased from Ted Pella, Inc. (Redding, CA, USA) with nominal diameters of 20, 50, 80, 100, and 150 nm, NIST Reference Material (RM) 8012 (Gold Nanoparticles, Nominal 30 nm Diameter), [38] and NIST RM 8013 (Gold Nanoparticles, Nominal 60 nm Diameter). [39] The mean diameter obtained with transmission electron microscopy (TEM), the particle number concentration, and the Au mass concentration of each of the NPs used in this work are presented in Table 1.

Instrumentation

A ThermoFisher X series 7 quadrupole ICP-MS (Thermo, Waltham, MA, USA) was used for ICP-MS and spICP-MS measurements. Samples were introduced into the ICP torch using a quartz C-Type nebulizer (Elemental Scientific, Omaha, NE, USA) and impact bead spray chamber cooled to 2 °C. The sample flow rate was set to approximately 0.5 mL min^{-1} and measured daily in triplicate by weighing the water uptake after 5 min. Daily tuning of the ICP-MS was accomplished for maximum ^{115}In sensitivity and minimum $^{156}CeO/^{140}Ce$ level (<2 %). Under these conditions, the ICP-MS also exhibited maximum sensitivity for ^{197}Au. A dwell time of 10 ms was used for all spICP-MS experiments, and ^{197}Au intensity was recorded in time-resolved analysis mode using ThermoFisher PlasmaLab software. Data were exported and processed manually in a spreadsheet. An IEC Centra CL2 ThermoFisher centrifuge, with a swinging bucket rotor accessory, was used for the SDGC.

Sucrose density gradient centrifugation of mixtures of AuNPs with different sizes

To explore the capabilities of SDGC at NP mass fractions in the sub ng g^{-1} level, three mixtures of AuNPs, each mixture containing three AuNP populations with three different nominal sizes (*Mixture 1*: 30, 60, and 100 nm; *Mixture 2*: 20, 50, and 100 nm; *Mixture 3*: 30, 80, and 150 nm), were studied in two different conditions [equal particle number concentration (ePNC) of 1.02×10^7 mL^{-1} for each component; and equal Au mass fraction (eMF) of 100 ng g^{-1} for each component]. The Au mass fractions of the components of the mixtures in the ePNC condition are given in Table S1 in the Electronic Supplementary Material (ESM). For the purpose of communication in this paper, the mixtures are sometimes referred to as either “resolved” or “unresolved.” These designations, obviously assigned to the mixtures after the data had been acquired, refer to the success of the size separation eventually achieved in these studies.

Sucrose solutions were prepared by dissolving the appropriate amount of pure sucrose in deionized water. Solutions were gently heated and stirred until completely dissolved. Food coloring (20 μL) was added to the stock sucrose solutions as a visual aid to discriminate the different layers having different contents of sucrose. For each experiment, the sucrose density gradient was carefully constructed from bottom to top with a transfer pipet, using a 15 mL plastic centrifuge tube as follows: 50 % sucrose (3 mL), 40 % sucrose (3 mL), 30 % sucrose (3 mL), 2 mL deionized water, and 2 mL of the particular mixture of AuNPs. (Johnson et al. 2016, *to be submitted to ACS Nano*) All sucrose contents are expressed as mass fractions.

Centrifugal separation of AuNP mixtures ($n = 4$) was performed at room temperature in a swinging bucket centrifuge under the following conditions: 10 min at 172 *g* followed by, and without interruption, 10 min at 1254 *g*. After centrifugation, 1 mL aliquots of each replicate were successively removed from each layer by pipet from the centrifuge tubes containing the sucrose density gradient samples. (Johnson et al. 2016, *to be submitted to ACS Nano*) The aliquots were designated from layer 13, corresponding to the top of the gradient composition, to layer 1 which represents the bottom most layer (see ESM Scheme S1A). Samples were weighed before total Au determination and the spICP-MS analysis in duplicate.

Determination of the total gold content in the sucrose layers by conventional ICP-MS

The determination of the total gold contents for the 1 mL samples extracted from the layers was performed in duplicate after room temperature digestion with 1 mL of aqua regia (3:1 HCl/HNO_3, volume fraction). After 1 h, the mixtures were diluted with 12 mL of an internal standard solution containing 1 ng g^{-1} each of platinum and indium in 1.5 % volume fraction HNO_3. Six gold calibration standards spanning the gold mass fraction range from 0.05 to 25 ng g^{-1} were prepared by serial dilution using the indium and platinum internal standard solution as the diluent. Procedural blanks with ultrapure water ($n = 5$), calibration standards, and sample digestions were analyzed by conventional ICP-MS under the following conditions: 90 s sample uptake; 3 replicate measurements at *m/z* 115, 195, and 197; 60 s acquisition time; 1000 sweeps per replicate; and 100 ms dwell time per isotope.

Single particle ICP-MS analysis

Following a calibration protocol for spICP-MS previously described, [40] the instrument transport efficiency was calibrated using the NIST reference materials 8012 and 8013, citrate stabilized AuNPs in aqueous suspension, after dilution to an approximate particle number concentration of 1.5×10^4 mL^{-1} (equivalent to Au mass fractions of 3.2 and 26.5 pg g^{-1}, respectively), and the instrument sensitivity was calibrated using dissolved Au standards.

To have fuller knowledge about the stock suspensions of all AuNPs involved in this study, each was characterized for mean size, size distribution, and particle number concentration using spICP-MS (see Table 1 and ESM Fig. S1). For this purpose, the nanoparticle suspensions were prepared in triplicate by gravimetric serial dilution with high-purity water to an approximate particle number concentration of 1.5×10^4 mL^{-1} (equivalent to Au mass fractions from 0.8 to 350 pg g^{-1}, depending on the diameter). Each prepared sample was analyzed three times for 360 s.

For the spICP-MS analyses of the 1 mL extracted layers, duplicate customized serial dilutions, based on the total gold concentrations previously determined, were carried out in order to operate within the spICP-MS linear range. Dilution factors ranging from 5×10^3 to 2×10^5 were employed. Each prepared sample was analyzed three times for 360 s. Following a strategy published by our group, a 20-fold reduced sensitivity was required to properly measure the 150 nm AuNPs. [36] All NP suspension samples for all studies reported were bath-sonicated for 4 min before spICP-MS measurement.

Results and discussion

Characterization of sucrose density gradient centrifugation by conventional ICP-MS

The separation capability of the sucrose density gradient exhibited in Scheme S1A was initially evaluated for *Mixture 1* containing 30 nm (NIST 8012), 60 nm (NIST 8013), and 100 nm AuNPs in the ePNC condition. Conventional ICP-MS was used to evaluate the distribution of Au across the sucrose layers after centrifugation times of 20, 40, and 60 min. As shown in ESM Fig. S2, a centrifugation time of 20 min resulted in what appeared to be the best separation. It is worth noting that in this ePNC condition the Au mass fraction for the 100 nm AuNPs is 6 and 50 times higher than that of the 60 and 30 nm AuNPs, respectively (see ESM Table S1). Therefore, it is expected that 100 nm AuNPs would be the dominant contribution regarding the total Au content. This assertion is evidenced by Fig. 1 and Fig. S2 (ESM), where a single large peak, most likely corresponding to 100 nm AuNPs, is seen.

The separation capability of the sucrose density gradient for *Mixture 1* was also tested in the eMF condition, for which the contribution of Au in three distinctive areas in the gradient was observed (see Fig. 1). This finding was examined further in a parallel experiment in which each component of *Mixture 1* was individually applied to a separate sucrose gradient at 100 μg L^{-1} Au mass fraction. The results (see ESM Fig. S3) revealed an inherent overlap among two or three different AuNP sizes in all layers. This confirmed that this sucrose density gradient was unable to completely achieve the physical separation of the components of this mixture, even at such extremely low mass fractions.

A quantitative mass balance for *Mixture 1* was obtained for total Au across the layers (Table 2) in both the ePNC and eMF conditions, demonstrating that the initial Au content contained in the original suspensions of AuNPs was quantitatively recovered after the centrifugation process. (Throughout this study, recoveries of 90 % or greater are considered quantitative.) The quantitative recoveries reveal that conventional ICP-MS plays a role in validating the efficacy of the centrifugal separation methodology. Nevertheless, it is important to stress that in both the ePNC and eMF conditions, total Au analysis provided no evidence of a physical separation of the components of *Mixture 1* across the sucrose density gradient.

An alternative gradient, presented in Scheme S1B (ESM) and composition found in the ESM, was employed to explore the possibility of improving the efficiency of separation of *Mixture 1* at both ePNC and eMF conditions. However, total gold analysis (ESM Fig. S4) showed a similar behaviour to previous gradient features, with no improvement in the efficiency of the separation for the new gradient. Therefore, the original gradient (ESM Scheme S1A) was employed thereafter.

spICP-MS size resolution and number quantification capabilities for “unresolved” mixtures: Mixture 1 and Mixture 2

Total Au analysis by conventional ICP-MS revealed a lack of physical separation of the three components of *Mixture 1.* The concentration of each component of AuNPs assayed was extremely low for examination by classical NP characterization techniques, such as dynamic light scattering (DLS), transmission and scanning electron microscopies (TEM and

SEM), UV–vis spectroscopy, atomic force microscopy (AFM), etc. This was confirmed after an attempt to characterize the AuNPs of the layers of the gradient by high resolution SEM. No NPs were detected for layers that contained the highest Au mass fractions in either the ePNC or eMF conditions (data not shown). Therefore, spICP-MS was anticipated to be an advantageous tool, because it is capable of simultaneously sizing and quantifying the components of NPs with different sizes at mass fraction levels down to sub pg g^{-1}.

Before performing spICP-MS analyses on samples derived from the sucrose density gradient centrifugation experiments, it was expedient to evaluate the performance of the specific spICP-MS measurement procedure to be used. To accomplish this, the mean diameter, size distribution, number concentration, and Au mass fraction recovery of each AuNP component, suspended in fresh water, used to prepare the mixtures was measured using the spICP-MS protocol. The results shown in Table 1 and Fig. S1 (ESM) show acceptable performance.

Based on previous total Au analysis results for *Mixture 1*, customized serial dilutions of 1 mL aliquots extracted from the gradient layers for the ePNC and eMF conditions were prepared to ensure operation within the linear range of spICP-MS, assuming one predominant AuNP component located in every layer. It should be stressed that while the conventional ICP-MS analysis results were helpful for estimating these customized dilution factors, such results were not strictly necessary. However, exclusive spICP-MS analysis would be laden with trial and error with respect to dilution factors for achieving the linear range, increasing the time and sample consumption and laboratory effort. After the dilutions had been performed, the AuNP number concentrations and size distributions were measured for the diluted samples, assuming monodisperse, spherical particles.

Figure 2a shows the results of the spICP-MS quantification of the particle number concentration of each AuNP size component in *Mixture 1* in every single layer of the sucrose density gradient after centrifugation. The data shown are for the ePNC condition. Note that the particle number concentration is expressed as recovery, calculated as the ratio of the AuNPs found in one layer to the total number of AuNPs loaded to the gradient, where the latter was estimated from the TEM mean size and the Au mass fraction provided in the Reports of Investigation [38, 39] or the specification reported by the supplier. To derive the results, it was necessary to decide which AuNP events observed in the spICP-MS data would correspond to each AuNP component population of the mixture. The size histograms generated for the individual AuNP component populations suspended in fresh water (ESM Fig. S1) were used for this purpose. Specifically, AuNPs in the ranges of 10 to 44 nm, 45 to 84 nm, and 85 to 120 nm were attributed to 30, 60, and 100 nm AuNPs, respectively. From the information in Fig. 2a, the 30 nm AuNPs are mainly confined to layers 13 to 10, with a smaller contribution in layers 9 to 7. The 60 nm AuNPs are mainly located in layers 10 to 8, but also are present through layers 13 to 11 and 7 to 6. However, the 100 nm AuNPs are found predominantly in layers 9 to 6, with significantly smaller quantities in layers 5 to 1. Note that the quantification of the particle number concentration carried out by spICP-MS for the 100 nm AuNPs was in good agreement with the total Au results obtained by conventional ICP-MS. Furthermore, spICP-MS allowed the quantification of 30 and 60 nm AuNPs in the ePNC condition, which was not feasible by the total Au approach.

The mass balance for the three components of *Mixture 1* is shown in Table 3. A quantitative recovery for 60 and 100 nm AuNPs was obtained; however, a recovery of only approximately 60 % was achieved for 30 nm AuNPs. We are unsure why the recovery was low in this case, but we believe it might be due to an inadvertent overdilution of the first layers of the gradient, which hampered the quantitative detection of the 30 nm AuNPs. This conjecture is supported by the spICP-MS size distributions for layers 13 through 11 presented in Fig. S5 in the ESM, which show relatively few AuNP events compared to the remaining layers where the larger AuNPs are mostly located.

The spICP-MS mean AuNP diameters observed in the layers are presented in Fig. 2b. Again, the lack of physical separation of the discrete AuNP sizes of *Mixture 1* along the gradient is evident. More detailed information about the relative contribution of each component to the total number of AuNPs detected in each layer and about the size distributions across the layers are presented in the ESM in Fig. S6 and Fig. S7, respectively.

The behavior of the separation of *Mixture 1* in the eMF condition within the gradient is exhibited in Fig. 3. The recovery for the 100 nm AuNPs was quantitative [from (114.6 ± 20.0) %; Table 3] and matched the profile found using the ePNC condition, since they were present at the same Au mass fraction. A cursory glance at Fig. 1 (solid line) would lead to the initial interpretation that there was a discrete separation of the three components. However, spICP-MS analysis revealed a possible misinterpretation of the total Au results for the distribution of 30 and 60 nm AuNPs across the gradient, since both AuNPs are present together with the same relative recovery in the first four layers (Fig. 3a). For *Mixture 1* in the eMF condition, it is worthwhile to note that for 30 nm AuNPs, the particle number concentration was a factor of 8 times and 46 times higher than for 60 and 100 nm AuNPs, respectively. This explains the prevalence of 30 nm AuNPs and the presence of some 60 nm AuNPs across all the layers (ESM Fig. S7 and Fig. S8). Figure 3b displays the variation of the mean size throughout the gradient using spICP-MS. Layers 13 to 10 convey the predominance of the 30 nm AuNPs; however, the influence of the 30 nm AuNPs can be noted in the bias towards a smaller mean size in the layers where larger AuNPs were located (7 and 6), causing an inversion of the trend in the last five layers. Again, a quantitative recovery of the particle number concentration was achieved for 60 and 100 nm AuNPs (Table 3). However, for the 30 nm AuNPs, a quantitative recovery was not possible (only ≈ 70 %) due to the existence of ≈ 5 % of agglomerates (from 145 to 200 nm) in the last five layers, which can be explained by the coexistence of the 30 nm AuNP in the layers containing larger particles.

Similar to *Mixture 1*, total Au analysis (ESM Fig. S9) revealed a “non-ideal” separation of the three components of *Mixture 2* for both the ePNC and eMF conditions. Details of the particle number concentration, the size distribution histograms of the components across the layers, the mean NP sizes observed in the layers, and the global recovery for both the ePNC and eMF conditions are displayed in the ESM from Fig. S10 to Fig. S13 and Table S2.

spICP-MS size resolution and number quantification capabilities for a “resolved” mixture: Mixture 3

The efficiency of the sucrose density gradient to separate an “ideal mixture” was finally assessed using *Mixture 3*. This mixture was designed to avoid the coexistence of the two smaller AuNPs of the mixtures, which previously hampered the proper evaluation of the gradient separation capacity.

Contrary to the scenarios previously described, a different total Au analysis profile was revealed in the ePNC condition, where at least a clear separation between the 80 and 150 nm AuNPs was obtained (ESM Fig. S14). However, total Au analysis still failed to provide information regarding the location of the 30 nm AuNPs within the gradient, due to the very low relative Au mass fraction in *Mixture 3* (175 times lower than 150 nm). As clearly shown in the spICP-MS recovery results (Fig. 4a), a far superior separation of the three components was achieved for *Mixture 3* in the ePNC condition. In this case, AuNPs in the ranges of 10 to 49 nm, 50 to 109 nm, and 110 to 199 nm were attributed to 30, 80, and 150 nm AuNPs, respectively. Evidenced by Fig. 4a, > 85 % of 30 nm AuNPs were confined to layers 13 to 10 where no traces of 80 nm AuNPs were found. In fact, 80 nm AuNPs were mainly located in layers 10 through 7 and the 150 nm AuNPs were found predominantly in layers 5 to 1. Interestingly, coexistence of a small amount of 80 nm and 150 nm AuNPs can be seen only in layer 6, the interface between the 30 and 40 % sucrose layers. Moreover, this practically total physical separation enables the acquisition of a quantitative recovery for all the components (Table 4). Corroborating the quantitative number concentration results, the size distribution histograms across the layers, presented in Fig. 5, provide a clear visualization of the practically total separation of the components of *Mixture 3*. (The relative contributions of each AuNP size to each layer are shown in ESM Fig. S15.) Notice the presence of three discrete plateaus in the plot of the variation of the mean AuNP size observed across the layers (Fig. 4b). Both results demonstrate the suitability of the SDGC approach to efficiently separate the components of *Mixture 3*. However, the most important point is that this key finding on the resolution power of the SDGC at such low AuNP concentration levels can only be addressed with spICP-MS detection.

Comparable to the ePNC condition, spICP-MS recovery showed an apparent physical resolution for the constituents of *Mixture 3* in the eMF condition (Fig. 6a), as well as a quantitative recovery for all sizes (Table 4). Quantitative recovery for the smaller AuNPs was finally achieved for *Mixture 3* in both conditions, implying not only an efficient separation, but also a lack of agglomeratation. It is important to stress that the particle number concentration of 30 nm AuNPs was a factor of 26 times and 175 times higher than for the 80 and 150 nm AuNPs, respectively. In this context, the presence of traces of 30 nm AuNPs found in denser layers, supported by the size histograms along the gradient (ESM Fig. S16) and the contribution of 30 nm AuNPs to the total number of NPs detected (ESM Fig. S17), impacted the mean size determined within those layers (Fig. 6b). This effect indicates an overwhelming of the separation capacity of the sucrose gradient for smaller NPs in such mixtures, where different NP sizes are present in a large range of particle number concentrations.

Conclusions

In this paper, the proof of concept of using spICP-MS to study the capabilities of SDGC for the separation of different AuNP mixtures at two environmentally relevant conditions (ePNC and eMF) has been demonstrated. We again emphasize that the NP concentrations studied here are those that might be found in actual environmental samples, and that using such low NP concentrations was made possible by the use of SDGC in tandem with the extremely good sensitivity of spICP-MS. In this respect, spICP-MS reflects a substantial advantage over conventional analytical techniques (e.g. UV–vis, dynamic light scattering, TEM, atomic force microscopy, differential mobility analysis, etc.), which are typically limited to providing information at higher concentration levels of NPs. Therefore, the results of this paper open greater possibilities of performing EHS studies on nanomaterials with truly meaningful results. It should also be noted that implementation of spICP-MS alone in such studies is not always advisable, due to the destructive nature of the technique. In contrast, SDGC in nondestructive, leaving the separated NPs available for further study.

In the NP-synthesis field, post-synthesis NP separation protocols are critical for achieving NP suspensions of discrete sizes and shapes, and aggregation control. These separation processes must be carefully developed, assessed for the efficacy of the physical separation/isolation of the components of interest, and suitably optimized/modified before long-term implementation. For this study, after customized dilutions of each individual layer of the gradient, spICP-MS was employed to measure AuNP size, size distribution, and particle number concentration in each layer, thereby delineating the contribution to each layer of each AuNP component of the three mixtures under study. Even in the event that conventional ICP-MS does not display evidence of a physical separation of the components, spICP-MS was able to characterize the AuNP size distribution within the SDGC separation. That was the case for *Mixture 1* and *Mixture 2*, whose three components exhibited a “non-ideal” separation pattern. spICP-MS size and particle number concentration results corroborated a lack of separation of the discrete AuNP sizes of both mixtures. These mixtures exhibited evidence of the coexistence of the two smaller AuNPs, which hampered a proper evaluation of the separation capacity.

In contrast, the sucrose density gradient proposed here was able to efficiently address the separation of *Mixture 3* (30, 80 and 150 nm) at a short centrifugation time (20 min). For this “ideal mixture” the presence of AuNPs with enough difference in mass and size resulted in a far superior separation in the ePNC condition, as proved by only spICP-MS. Unlike *Mixture 1* and *Mixture 2*, a quantitative recovery of particle number concentration was obtained for all three components of *Mixture 3* in both conditions (ePNC and eMF), which reinforces the suitability of spICP-MS to properly assess the efficiency of this SDGC method.

It is important to note that in the eMF condition, used in many research efforts, the presence of traces of smaller AuNPs in denser layers impacted the mean size and the size distribution in all mixtures. This fact indicates that the separation capacity of the sucrose gradient for smaller NPs is overwhelmed at higher particle number concentrations, which may have important implications for current practical applications.

The results from this study might be further applied toward the separation and/or characterization of complex mixtures of NPs in many relevant fields, such as environmental nanotechnology, NP-organism uptake studies, (Johnson et al. 2016, *to be submitted to ACS Nano*) waste water treatments, and quality control of consumer products, etc. This approach also opens the door to further research into the evaluation of mixtures of NPs of different elemental composition, taking advantage of the multi-elemental capability of spICP-MS. Additional experiments are needed to optimize the sucrose density gradient composition to reconcile between a total physical separation of NPs at extremely low levels and centrifugation time.

Acknowledgments

The authors wish to acknowledge Karen E. Murphy (National Institute of Standards and Technology, Gaithersburg, MD, USA) for the use of instrumentation and equipment.

References

1. Leitch ME, Casman E, Lowry GV. J Nanopart Res. 2012; 14:1283–9.
2. Peer D, Karp JM, Hong S. Nat Nanotechnol. 2007; 2:752–60.
3. Anker JN, Hall WP, Lyandres O. Nat Mater. 2008; 7:442–53. [PubMed: 18497851]
4. Sun BQ, Marx E, Greenham NC. Nano Lett. 2003; 3:961–3.
5. International Organization for Standardization (ISO). ISO TS 27687. 2008.
6. Sun YG, Xia YN. Science. 2002; 298:2176–9. [PubMed: 12481134]
7. Manna L, Scher EC, Alivisatos AP. J Am Chem Soc. 2000; 122: 12700–6.
8. Walker DA, Browne KP, Kowalczyk B, Grzybowski BA. Angew Chem Int Ed. 2010; 49:6760–3.
9. Klajn R, Pinchuk AO, Schatz GC, Grzybowski BA. Angew Chem Int Ed. 2007; 46:8363–7.
10. Tao F, Grass ME, Zhang YW. J Am Chem Soc. 2010; 132:8697–703. [PubMed: 20521788]
11. Yan JM, Zhang XB, Akita T. J Am Chem Soc. 2010; 132:5326–7. [PubMed: 20345145]
12. Mazumder V, Chi MF, More KL, Sun SH. J Am Chem Soc. 2010; 132:7848–9. [PubMed: 20496893]
13. Kang YJ, Murray CB. J Am Chem Soc. 2010; 132:7568–9. [PubMed: 20469855]
14. Sun X, Tabakman SM, Seo W-S, Zhang G, Sherlock S, Bai L, et al. Angew Chem Int Ed. 2009; 48:939–42.
15. Yin YD, Alivisatos AP. Nature. 2005; 437:664. [PubMed: 16193041]
16. Burda C, Chen X, Narayanan R, El-Sayed MA. Chem Rev. 2005; 105:1025. [PubMed: 15826010]
17. James CN, Novak P, Franzen S, Feldheim DL. Anal Chem. 2001; 73:5758. [PubMed: 11774918]
18. McLeod MC, Anand M, Kitchens CL, Roberts CB. Nano Lett. 2005; 5:461. [PubMed: 15755095]
19. Arnold MS, Stupp SI, Hersam MC. Nano Lett. 2005; 5:713. [PubMed: 15826114]
20. Kowalczyk B, Lagzi I, Grzybowski BA. Curr Opin Colloid Interface Sci. 2011; 16:135–48.
21. Brakke MK. Density Gradient Centrifugation and its Application to Plant Viruses. Advances in Virus Research. 1960:193–224.
22. Xiong B, Cheng J, Qiao Y, Zhou R, He Y, Yeung ES. 2011; 1218: 3823–3929.
23. Chen G, Wang Y, Tan LH, Yang MX, Tan LS, Chen Y, et al. J Am Chem Soc. 2009; 131:4218–9. [PubMed: 19275162]
24. Yanagi K, Iitsuka T, Fujii S, Kataura H. J Phys Chem. 2008; 112: 18889–94.
25. Zhang Y, Shi Y, Liou Y-H, Sawvel AM, Sun H, Cai Y, et al. J Mater Chem. 2010; 20:4162–7.
26. Lee SH, Salunke BK, Kim BS. Biotechnol Bioprocess Eng (find abbreviation). 2014; 19:169–174.
27. Mohan N, Chen CS, Hsieh HH, Wu YC, Chang HC. Nano Lett. 2010; 10:3692–9. [PubMed: 20677785]

28. Domingos RF, Baalousha MA, Ju-Nam Y, Reid MM, Tufenkji N, Lead JR, et al. Environ Sci Technol. 2009; 43:7277–84. [PubMed: 19848134]
29. Pettibone JM, Gigault J, Hackley VA. ACS Nano. 2013; 7:2491–9. [PubMed: 23425128]
30. Montoro Bustos AR, Ruiz Encinar J, Sanz-Medel A. Anal Bioanal Chem. 2013; 405:5637–43. [PubMed: 23681200]
31. Delguedre C, Favarger PY, Wold S. Anal Chim Acta. 2006; 555: 263–8.
32. Laborda F, Bolea E, Jimenez-Lamana J. Anal Chem. 2014; 86: 2270–8. [PubMed: 24308527]
33. Montoro Bustos AR, Petersen EJ, Possolo A, Winchester M. Anal Chem. 2015; 87:8809–17. [PubMed: 26265147]
34. Sadik OA, Du N, Kariuki V, Okello W, Bushlyar V. ACS Sustain Chem Eng. 2014; 2:1707–16.
35. Laborda F, Jimenez-Lamana J, Bolea E, Castillo JR. J Anal At Spectrom. 2011; 26:1362–71.
36. Liu J, Murphy KE, MacCuspie RI, Winchester MR. Anal Chem. 2014; 86:3405–14. [PubMed: 24575780]
37. Mitrano DM, Barber A, Bednar A, Westerhoff P, Higgins CP, Ranville JF. J Anal At Spectrom. 2012; 27:1131–42.
38. Report of Investigation for Reference Material 8012, Gold Nanoparticles, Nominal 30 nm Diameter. National Institute of Standards and Technology; Gaithersburg: 2012.
39. Report of Investigation for Reference Material 8013, Gold Nanoparticles, Nominal 60 nm Diameter. National Institute of Standards and Technology; Gaithersburg: 2012.
40. Pace HE, Rogers NJ, Jarolimek C, Coleman VA, Higgins CP, Ranville JF. Anal Chem. 2011; 83:9361–9. [PubMed: 22074486]

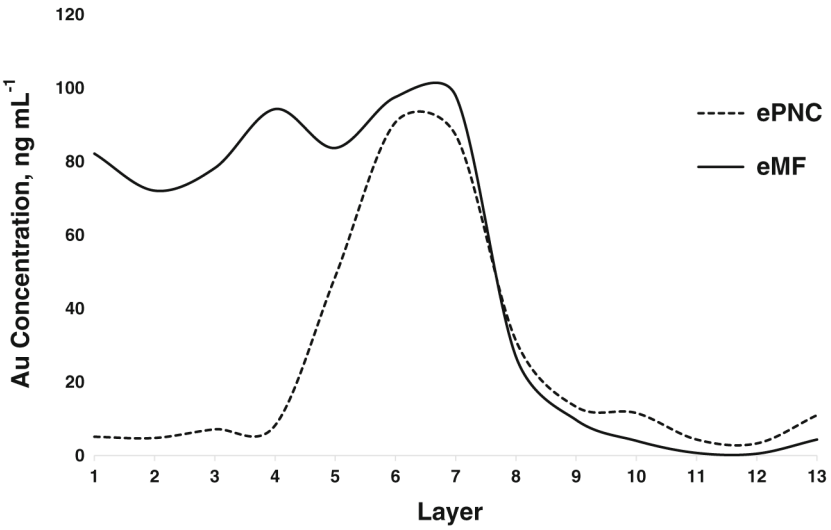

Fig. 1.

Distribution of gold across the layers of the sucrose density gradient for *Mixture 1* containing 30, 60, and 100 nm AuNPs by conventional ICP-MS after 20 min of centrifugation. Total gold content in individual 1 mL aliquots are plotted from the top of the conical tube to the bottom in the eMF (*solid line*) and ePNC (*dotted line*) conditions, respectively

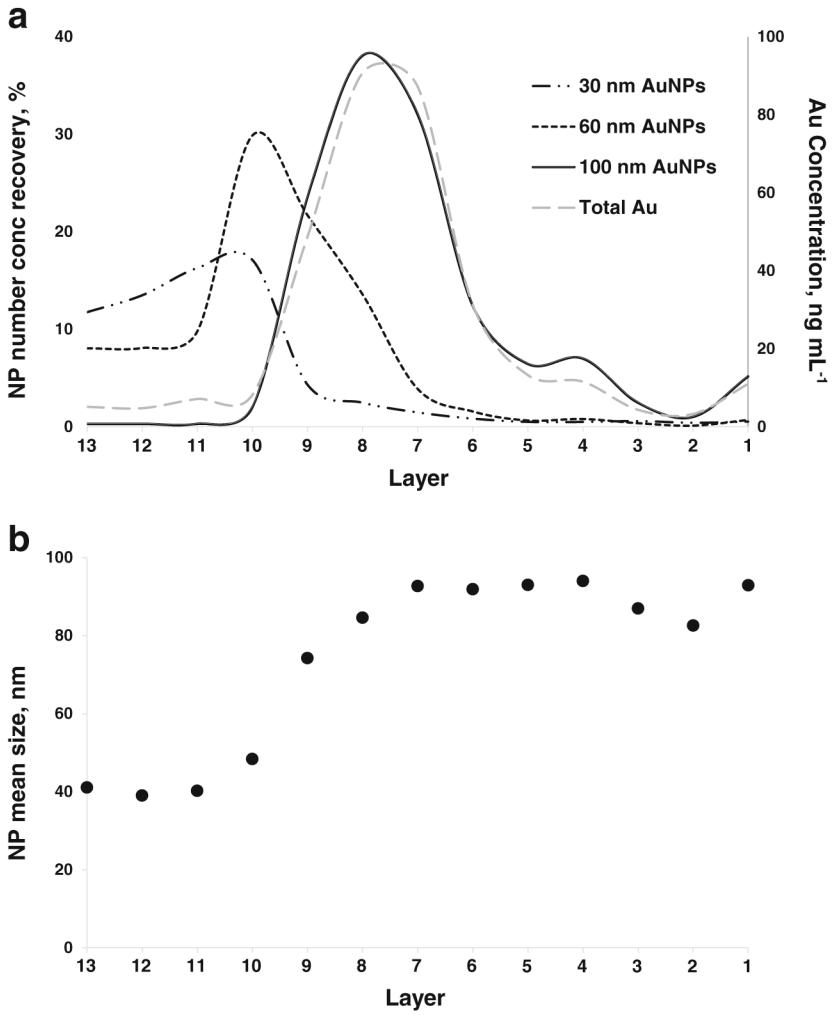

Fig. 2.

a AuNP number concentration recovery of the components of *Mixture 1* across layers of the sucrose density gradient in the ePNC condition by spICP-MS. Long *dash dotted line* corresponds to 30 nm AuNPs, *dotted line* plots the 60 nm AuNPs and the solid line reflects the 100 nm AuNPs. The *gray dashed line* and the secondary axis correspond to the distribution of gold obtained by conventional ICP-MS. **b** Mean AuNP size in each layer measured using spICP-MS

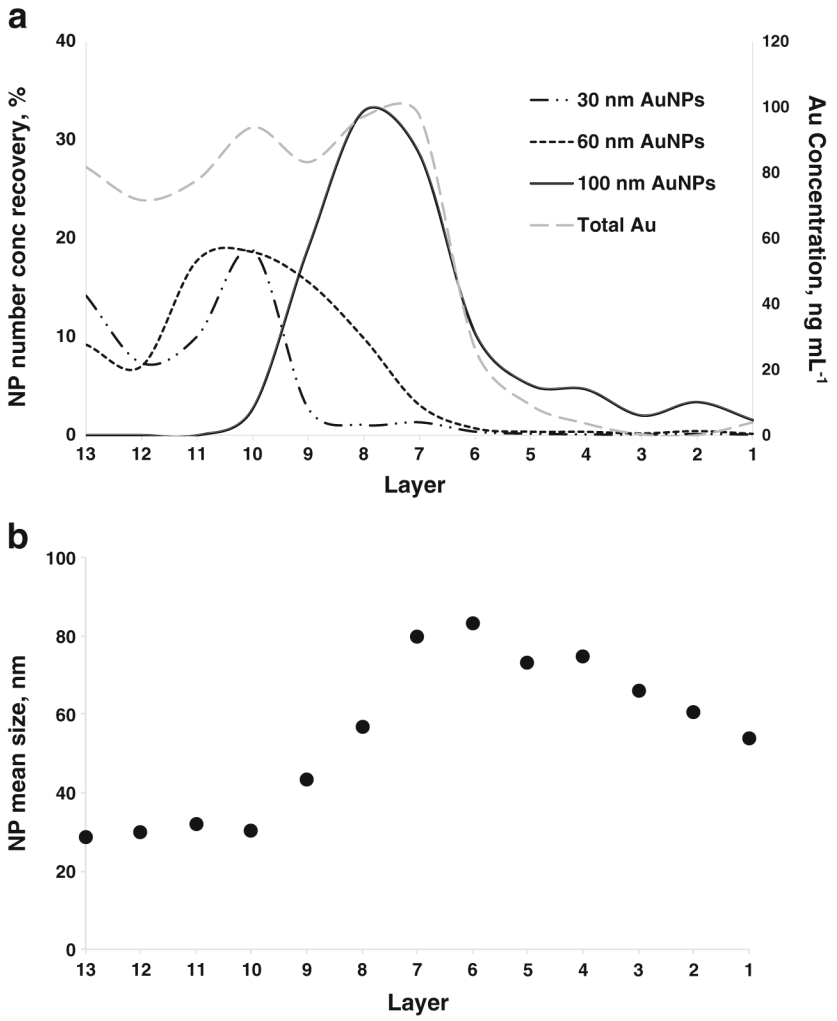

Fig. 3.

a AuNP number concentration recovery of the components of *Mixture 1* across layers of the sucrose density gradient in the eMF condition by spICP-MS. Long *dash dotted line* corresponds to 30 nm AuNPs, *dotted line* plots the 60 nm AuNPs and the solid line reflects the 100 nm AuNPs. The *gray dashes line* and the secondary axis correspond to the distribution of gold obtained by conventional ICP-MS. **b** Mean AuNP size in each layer measured using spICP-MS

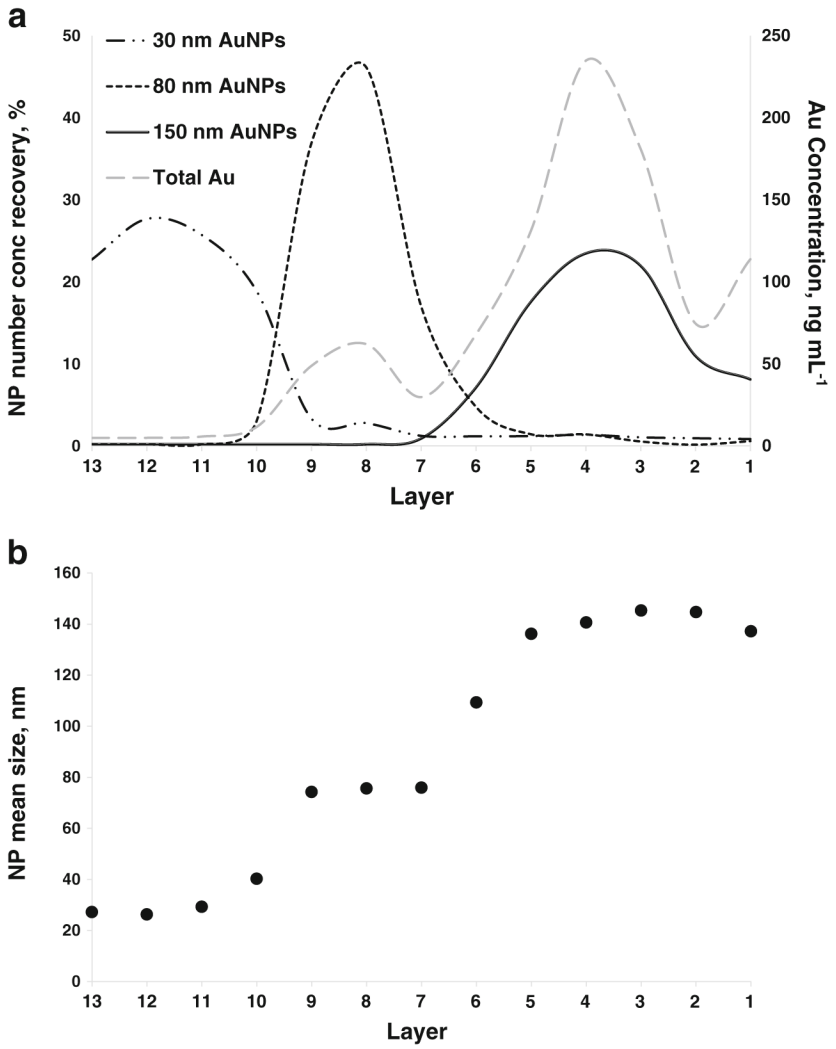

Fig. 4.

a AuNP number concentration recovery of the components of *Mixture 3* across layers of the sucrose density gradient in the ePNC condition by spICP-MS. Long *dash dotted line* corresponds to 30 nm AuNPs, *dotted line* plots the 80 nm AuNPs and the *solid line* reflects the 150 nm AuNPs. The *gray dashed line* and the secondary axis correspond to the distribution of gold obtained by conventional ICP-MS. **b** Mean AuNP size in each layer measured using spICP-MS

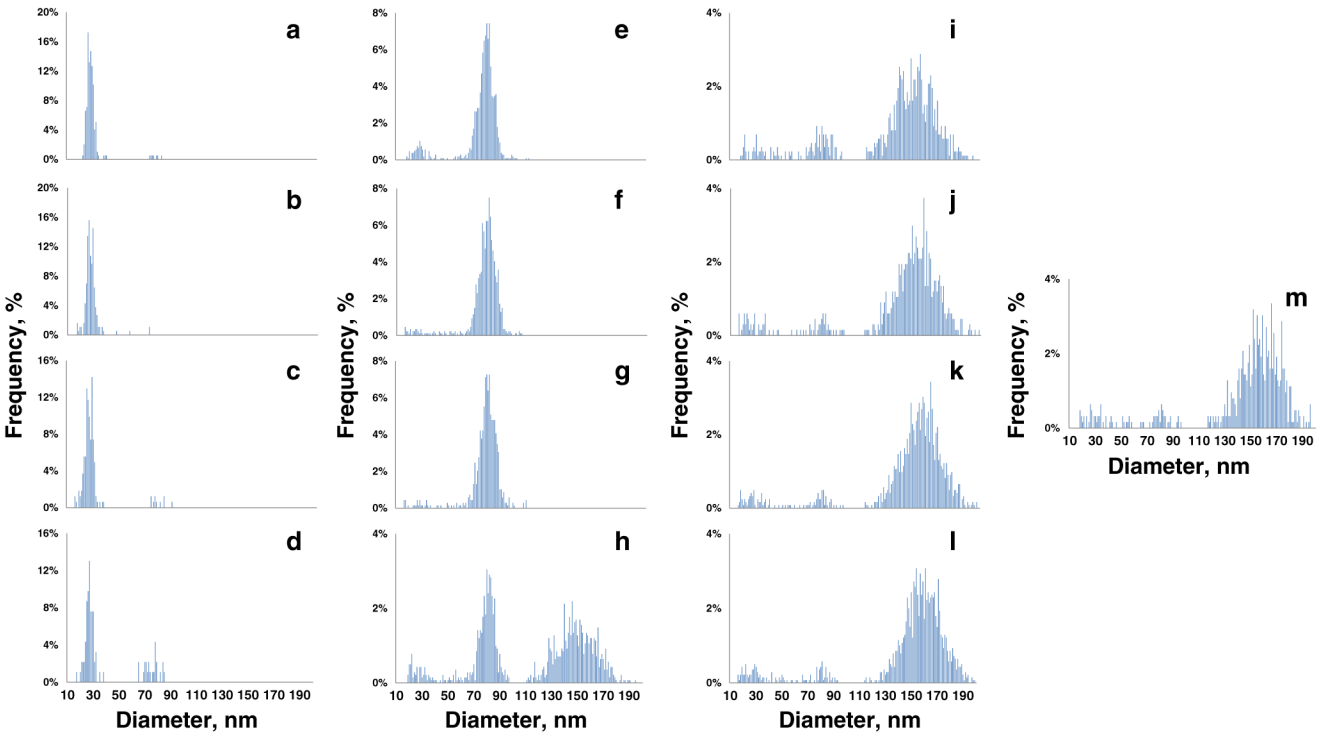

Fig. 5.

Size distribution histograms measured by spICP-MS for *Mixture 3* in the ePNC condition across the layers of the sucrose density gradient. Layers from 13 to 1 are displayed from A to M, respectively

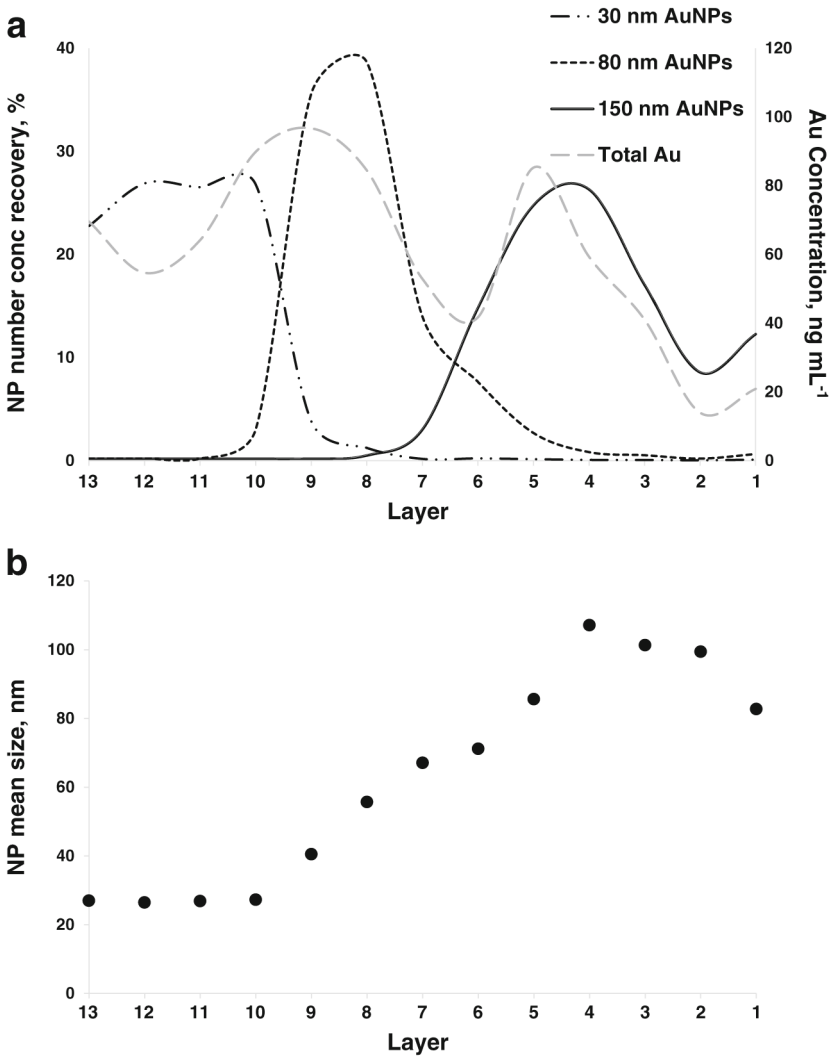

Fig. 6.

a AuNP number concentration recovery of the components of *Mixture 3* across layers of the sucrose density gradient in the eMF conditions by spICP-MS. Long *dash dotted line* corresponds to 30 nm AuNPs, *dotted line* plots the 80 nm AuNPs and the solid line reflects the 150 nm AuNPs. The *gray dashed line* and the secondary axis correspond to the distribution of gold obtained by conventional ICP-MS. **b** Mean AuNP size in each layer measured using spICP-MS

Table 1

Comparison of Average Particle Size Measured by spICP-MS to the TEM results provided by the supplier. Particle Number Concentration and Au concentration recovery determined by spICP-MS

AuNP	Au Conc., μg mL^{-1} [a]	NP Number Concentration NP mL^{-1} [b]	TEM Diameter (nm)[c]	spICP-MS Diameter (nm)[c]	spICP-MS NP Number & Au Conc. Recovery (%)[c]
NIST RM 8012,30 nm	48.17 [d]	2.3×10^{11}	27.6 ± 2.1[e]	26.8 ± 3.3	100.3 ± 2.2
NIST RM 8013,60 nm	51.86 [d]	2.9×10^{10}	56.0 ± 0.5[e]	55.3 ± 6.2	101.7 ± 4.1
20 nm	56.60	7.0×10^{11}	20.3 ± 1.6	20.5 ± 2.9	85.0 ± 4.8
50 nm	56.80	4.6×10^{10}	49.7 ± 3.9	48.3 ± 5.3	95.5 ± 3.2
80 nm	56.69	1.1×10^{10}	80.1 ± 6.3	78.0 ± 7.1	95.8 ± 6.6
100 nm	56.60	5.8×10^{9}	98.9 ± 7.8	95.8 ± 6.6	102.4 ± 2.0
150 nm	56.60	1.7×10^{9}	149.9 ± 11.8	154.2 ± 15.2	100.6 ± 3.2

[a] Information provided by NIST Reports of Investigation [38, 39] for RM 8012 and RM 8013 and consumer specification from Ted Pella, Inc. for the 20, 50, 80, 100, and 150 nm AuNPs

[b] Value obtained using the Au concentration and TEM mean diameter, assuming monodispersed, spherical particles

[c] Uncertainties correspond to single standard deviations of multiple determinations

[d] Mass fraction expressed as μg g^{-1}

[e] Expanded uncertainty of the mean for 95 % coverage, but only measurement repeatability was accounted for

Table 2

Mass balance (%) of the total Au for all the mixtures after SDGC determined by conventional ICP-MS in the ePNC and eMF conditions. Each datum is expressed as the ratio of the sum of the Au content found in every layer to the initial Au content contained in the suspension of AuNPs introduced to the gradient

Mixture	ePNC (%)	eMF (%)
Mixture 1	104.4 ± 9.0	98.2 ± 2.3
Mixture 2	103.1 ± 5.2	95.9 ± 0.8
Mixture 3	95.8 ± 9.6	95.2 ± 1.1

Uncertainties correspond to single standard deviations

Table 3

Recovery (%) for the particle number concentration of the three components of *Mixture 1* after SDGC determined by spICP-MS in the ePNC and eMF conditions

AuNPs	ePNC (%)	eMF (%)
30 nm	59.3 ± 4.3	69.9 ± 0.7
60 nm	90.1 ± 9.8	92.8 ± 9.0
100 nm	110.3 ± 12.0	114.6 ± 20.0

Uncertainties correspond to single standard deviations

Table 4

Recovery (%) for the particle number concentration of the three components of *Mixture 3* after SDGC determined by spICP-MS in the ePNC and eMF conditions

AuNPs	ePNC (%)	eMF (%)
30 nm	101.7 ± 10.1	104.3 ± 6.4
80 nm	103.3 ± 7.9	100.8 ± 0.8
150 nm	89.7 ± 0.8	103.7 ± 3.2

Uncertainties correspond to single standard deviations